

## ***Ab initio* determination of the $P$ - and $T$ -violating coupling constants in atomic Xe by the relativistic-coupled-cluster method**

Yashpal Singh,<sup>1</sup> B. K. Sahoo,<sup>1,\*</sup> and B. P. Das<sup>2</sup>

<sup>1</sup>*Theoretical Physics Division, Physical Research Laboratory, Navrangpura, Ahmedabad 380009, India*

<sup>2</sup>*Theoretical Physics and Astrophysics Group, Indian Institute of Astrophysics, Bangalore 560034, India*

(Received 10 December 2013; published 31 March 2014)

The parity ( $P$ ) and time-reversal ( $T$ ) odd coupling constant associated with the tensor-pseudotensor (T-PT) electron-nucleus interaction and the nuclear Schiff moment (NSM) have been determined by combining the result of the measurement of the electric dipole moment (EDM) of a  $^{129}\text{Xe}$  atom and our calculations based on the relativistic-coupled-cluster (RCC) theory. Calculations using various relativistic many-body methods have been performed at different levels of approximation. The accuracies of our results are estimated by comparing our dipole polarizability calculations of the ground state of Xe with its most precise available experimental data, and taking into consideration the difference of the results of our RCC single- and double-excitation calculations with and without the important triple excitations as well as the size of our basis set. The nonlinear terms that arise in the RCC theory were found to be crucial for achieving high accuracy in the calculations. We obtain the upper limits for the T-PT electron-nucleus coupling coefficient and NSM as  $1.6 \times 10^{-6}$  and  $1.2 \times 10^{-9} e \text{ fm}^3$ , respectively, by combining our calculations with the available measurement. Our results, in combination with future EDM measurements in atomic Xe, could improve these limits further.

DOI: [10.1103/PhysRevA.89.030502](https://doi.org/10.1103/PhysRevA.89.030502)

PACS number(s): 31.30.jp, 11.30.Er, 24.80.+y, 31.15.ve

The search for the electric dipole moment (EDM) is now in its seventh decade [1,2]. The observation of an EDM of an elementary particle or a composite system would be an unambiguous signature of the violations of parity ( $P$ ) and time-reversal ( $T$ ) symmetries.  $T$  violation implies a charge conjugation-parity ( $CP$ ) violation via the  $CPT$  theorem [3]. The standard model (SM) of elementary particle physics provides explanations for the experimentally observed hadronic  $CP$  violation in the decays of neutral K [4] and B [5–7] mesons, but the amount of  $CP$  violation predicted by the SM is not sufficient to account for the matter-antimatter asymmetry in the Universe [8]. The current limits for  $CP$ -violating coupling constants deduced from the atomic EDMs are several orders of magnitude higher than the predictions of these quantities by the SM [9–11]. In addition, atomic EDMs can probe  $CP$  violation originating from leptonic, semileptonic, and hadronic  $CP$  sources. Combining atomic EDM measurements with high-precision many-body calculations, it is possible to obtain various  $CP$ -violating coupling constants at the levels of the nucleus and the electron. Newly proposed EDM experiments on diamagnetic and paramagnetic atoms hold the promise of improving the sensitivity of the current measurements by at least a few orders of magnitude [12–16]. The EDMs of diamagnetic atoms arise predominantly from the electron-nucleus tensor-pseudotensor (T-PT) interaction and interaction of electrons with the nuclear Schiff moment (NSM) [17]. The electron-nucleus T-PT interaction is due to the  $CP$ -violating electron-nucleon interactions which translates into  $CP$ -violating electron-quark interactions at the level of elementary particles. The NSM, on the other hand, could exist due to  $CP$ -violating nucleon-nucleon interactions and the EDM of nucleons, and both of them in turn could originate from  $CP$ -violating quark-quark interactions or EDMs and

chromo EDMs of quarks. In order to obtain precise limits for the coupling constants of these interactions and EDMs of quarks, it is necessary to perform both experiments and calculations as accurately as possible on suitable atoms.

To date, the best limit for a diamagnetic atomic EDM is obtained from the  $^{199}\text{Hg}$  atom as  $d_A < 3.1 \times 10^{-29} e \text{ cm}$  [18] and the next best limit comes from an earlier measurement on the  $^{129}\text{Xe}$  atom as  $d_A < 4.1 \times 10^{-27} e \text{ cm}$  [19]. Both  $^{129}\text{Xe}$  and  $^{199}\text{Hg}$  isotopes are good choices for carrying out EDM measurements as they have nuclear spin  $I = 1/2$  and therefore the interaction with the octupole moment vanishes. Owing to the fact that the matrix elements of the T-PT and NSM interaction Hamiltonians increase with the atomic number ( $Z$ ) of the system [20], their enhancements in Hg are larger than those in Xe. However, the new proposals on EDM measurements in  $^{129}\text{Xe}$  argue in favor of carrying out the experiment in this isotope because of its larger spin relaxation time [13]. As a matter of fact, three research groups around the world are now actively involved in Xe EDM experiments [13,21,22]. Inoue *et al.* have proposed to utilize the nuclear-spin maser technique [23] to surpass the limit provided by the Hg EDM measurement.

In this Rapid Communication, we report the results of our systematic theoretical studies of the  $P$  and  $T$  odd coupling constant for the T-PT interaction and of the NSM in  $^{129}\text{Xe}$ . To this end, we have developed many-body methods in the framework of the third-order many-body perturbation theory [MBPT(3)] for a better understanding of the different classes of correlation effects, the coupled-perturbed-Hartree-Fock (CPHF) method in order to reproduce the previously reported results, and the relativistic-coupled-cluster (RCC) theory to bring to light the roles of both the CPHF and non-CPHF contributions (e.g., pair-correlation effects) to all orders in the residual Coulomb interaction (the difference between the exact two-body Coulomb and the mean-field interactions). In the present work, we consider one hole–one particle and

\*bijaya@prl.res.in

two hole–two particle excitations, i.e., the coupled-cluster theory with single and double excitations (CCSD) method and its linearized approximation, the LCCSD method. We also supplement the CCSD by an important subset of triple excitations. The ground state of a closed-shell atom such as Xe can be exactly described in the RCC theory by

$$|\Psi\rangle = e^T |\Phi_0\rangle, \quad (1)$$

where the cluster operator  $T$  generates all possible excitations from the Dirac-Hartree-Fock (DF) wave function  $|\Phi_0\rangle$ . However, if  $T = T_1 + T_2$ , then this approximation corresponds to the CCSD method. These operators can be expressed in second quantization notation using the hole and particle creation and annihilation operators as

$$T_1 = \sum_{a,p} a_p^\dagger a_a t_a^p \quad \text{and} \quad T_2 = \frac{1}{4} \sum_{a,b,p,q} a_p^\dagger a_q^\dagger a_b a_a t_{ab}^{pq}, \quad (2)$$

where  $t_a^p$  and  $t_{ab}^{pq}$  are the excitation amplitudes from the occupied orbitals denoted by  $a, b$  to the unoccupied orbitals denoted by  $p, q$  which embody correlation effects among the electrons to all orders.

We consider the Dirac-Coulomb (DC) Hamiltonian which in atomic units (a.u.) is given by

$$H = \sum_i \left[ c\alpha_D \cdot \mathbf{p}_i + (\beta_D - 1)c^2 + V_n(r_i) + \sum_{j>i} \frac{1}{r_{ij}} \right], \quad (3)$$

where  $c$  is the velocity of light in vacuum,  $\alpha_D$  and  $\beta_D$  are the Dirac matrices,  $V_n$  denotes the nuclear potential obtained using the Fermi-charge distribution, and  $\frac{1}{r_{ij}}$  is the dominant interelectronic Coulombic repulsion. We also take into account one order of an additional operator  $H_{\text{add}}$  which is either the dipole operator  $D$  for the evaluation of dipole polarizability ( $\alpha$ ) or the  $P$ - and  $T$ -violating interaction Hamiltonians for determining their corresponding coupling coefficients. The T-PT and the NSM interaction Hamiltonians are given by [24,25]

$$H_{\text{EDM}}^{\text{TPT}} = \frac{iG_F C_T}{\sqrt{2}} \sum \boldsymbol{\sigma}_n \cdot \boldsymbol{\gamma}_D \rho_n(r) \quad (4)$$

and

$$H_{\text{EDM}}^{\text{NSM}} = \frac{3\mathbf{S} \cdot \mathbf{r}}{B_4} \rho_n(r), \quad (5)$$

respectively, with  $G_F$  is the Fermi coupling constant,  $C_T$  is the T-PT coupling constant,  $\boldsymbol{\sigma}_n = \langle \sigma_n \rangle \frac{1}{I}$  is the Pauli spinor of the nucleus for the nuclear spin  $I$ ,  $\boldsymbol{\gamma}_D$  represents the Dirac matrices,  $\rho_n(r)$  is the nuclear density,  $\mathbf{S} = S \frac{1}{I}$  is the NSM, and  $B_4 = \int_0^\infty dr r^4 \rho_n(r)$ .

To distinguish between the correlations only due to the Coulomb and the combined Coulomb and the additional interaction, we further define

$$T = T^{(0)} + T^{(1)} \quad (6)$$

for the cluster operators  $T^{(0)}$  and  $T^{(1)}$  that account for the correlations only due to the Coulomb interaction and the combined Coulomb-additional interactions, respectively. To ensure the inclusion of only one order of the additional interaction in the wave function, we express

$$|\Psi\rangle \simeq (e^{T^{(0)}} + e^{T^{(0)}} T^{(1)}) |\Phi_0\rangle = |\Psi^{(0)}\rangle + |\Psi^{(1)}\rangle, \quad (7)$$

where  $|\Psi^{(0)}\rangle$  and  $|\Psi^{(1)}\rangle$  are the unperturbed and the first-order perturbed wave functions due to the additional interaction. Owing to the nature of the additional operators, the first-order perturbed wave function is an admixture of both the even and odd parities. The working equations for evaluating the excitation amplitudes of these RCC operators are described in Ref. [26].

Using the generalized Bloch equation, we can also express [26]

$$|\Psi\rangle = \Omega^{(0)} |\Phi_0\rangle + \Omega^{(1)} |\Phi_0\rangle = \sum_k [\Omega^{(k,0)} + \Omega^{(k,1)}] |\Phi_0\rangle, \quad (8)$$

where the  $\Omega$ 's are known as the wave operators with  $\Omega^{(0,0)} = 1$  and  $\Omega^{(1,0)} = H_{\text{add}}$  and  $k$  represents the order of interactions due to the Coulomb repulsion.

We also consider contributions from the important triple excitations in our calculations perturbatively (CCSD<sub>p</sub>T method) using the operator

$$\Omega_{\text{abg} \rightarrow \text{pqr}}^{\text{pert}} = \frac{\sum_s \langle pr | \frac{1}{r_{ij}} | sg \rangle \Omega_{\text{ab} \rightarrow \text{sq}}^{(\infty,0)} + \sum_c \langle cr | \frac{1}{r_{ij}} | ag \rangle \Omega_{\text{bc} \rightarrow \text{qp}}^{(\infty,0)}}{\epsilon_a + \epsilon_b + \epsilon_g - \epsilon_p - \epsilon_q - \epsilon_r}, \quad (9)$$

where  $\epsilon$ 's are the orbital energies and  $a \rightarrow p$  represents replacement of the occupied orbital  $a$  by a virtual orbital  $p$  in  $|\Phi_0\rangle$ . In the MBPT(3) method, we restrict  $k$  up to 2. The diagrams that make important contributions in this approximation are given explicitly in Ref. [26]. While in the CPHF method, we consider  $\Omega^{(k,0)} \approx \Omega^{(0,0)}$  and  $\Omega^{(k,1)}$  is evaluated to infinite order by restricting it only to one-hole–one-particle excitations by defining

$$\Omega_{a \rightarrow p}^{(\infty,1)} = \sum_{k=1}^{\infty} \sum_{b,q} \left\{ \frac{[\langle pb | \frac{1}{r_{ij}} | aq \rangle - \langle pb | \frac{1}{r_{ij}} | qa \rangle] \Omega_{b \rightarrow q}^{(k-1,1)}}{\epsilon_a - \epsilon_p} + \frac{\Omega_{b \rightarrow q}^{(k-1,1)\dagger} [\langle pq | \frac{1}{r_{ij}} | ab \rangle - \langle pq | \frac{1}{r_{ij}} | ba \rangle]}{\epsilon_a - \epsilon_p} \right\}, \quad (10)$$

with  $\Omega_{a \rightarrow p}^{(0,1)} = -\frac{\langle p | H_{\text{add}} | a \rangle}{\epsilon_p - \epsilon_a}$ .

Using the many-body tools discussed above, we evaluate  $X$  representing polarizability  $\alpha$ ,  $\eta = \frac{d_A}{\langle \sigma_N \rangle C_T}$ , or  $\zeta = \frac{d_A}{S / (|e| f m^3)}$  by considering the appropriate additional operator using the general expression

$$X = 2 \frac{\langle \Psi^{(0)} | D | \Psi^{(1)} \rangle}{\langle \Psi^{(0)} | \Psi^{(0)} \rangle}. \quad (11)$$

In the MBPT(3) method, we have

$$X = 2 \frac{\sum_{k=0}^{m=k+1,2} \langle \Phi_0 | \Omega^{(m-k-1,0)\dagger} D \Omega^{(k,1)} | \Phi_0 \rangle}{\sum_{k=0}^{m=k+1,2} \langle \Phi_0 | \Omega^{(m-k-1,0)\dagger} \Omega^{(k,0)} | \Phi_0 \rangle}. \quad (12)$$

Therefore, the lowest-order MBPT(1) with  $k = 0$  corresponds to the DF approximation and the intermediate MBPT(2) approximation follows with  $k = 1$ .

The above expression yields the forms  $X = 2 \langle \Phi_0 | \{ D \Omega^{(\infty,1)} \}_{\text{con}} | \Phi_0 \rangle$  in the CPHF method and  $X = 2 \langle \Phi_0 | \{ \widehat{D} T^{(1)} \}_{\text{con}} | \Phi_0 \rangle$  in the RCC theory with  $\widehat{D} = (1 + T^{(0)\dagger}) D$  in the LCCSD method and  $\widehat{D} = e^{T^{(0)\dagger}} D e^{T^{(0)}}$  is a nontruncating series in the CCSD and CCSD<sub>p</sub>T methods.

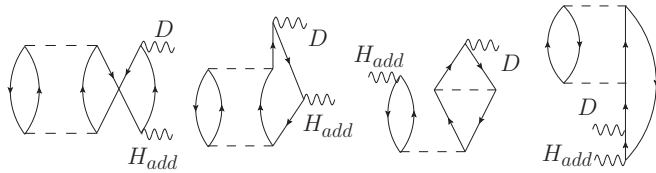


FIG. 1. Example of a few dominant non-CPHF diagrams from the MBPT(3) method involving  $D$  and the corresponding perturbed interaction operator  $H_{\text{add}}$ .

The subscript “con” implies that all the terms inside the curly bracket are connected. We have described in an earlier work the procedure for evaluating the diagrams that make the dominant contributions to  $\overline{D}$  [26].

We calculate  $\alpha$  for the ground state of Xe by the methods mentioned above to test their accuracies. The most precise measured value of this quantity is reported as  $27.815(27)ea_0^3$  [27]. In Table I, we present the calculated  $\alpha$ ,  $\eta$ , and  $\zeta$  values along with the experimental and previously reported results. As can be seen from this table, the DF result for  $\alpha$  is close to the experimental result, but this is not the case when correlation effects are added via the MBPT(2) and MBPT(3) methods. The results of the all-order CPHF, LCCSD, CCSD, and CCSD<sub>p</sub>T methods are in good agreement with the measured value, but the CCSD<sub>p</sub>T result is more accurate than the former methods. The rationale for considering the nonlinear RCC terms in the singles and doubles approximation supplemented by important triple excitations for the precise evaluation of the ground-state properties in Xe atom can be attributed to the non-negligible contributions from the non-RPA diagrams, as have been explicitly demonstrated in our earlier study on the polarizabilities of the closed-shell atomic systems [26]. It is also significant to note that the EDM enhancement factors exhibit different correlation trends than those of polarizability. The results increase gradually from the DF level after the inclusion of the correlation effects in the passage from the MBPT to LCCSD, and after that they decrease at the CCSD level. The uncertainties in our calculations are estimated by taking the difference between the CCSD and CCSD<sub>p</sub>T methods and from the incompleteness in

TABLE I. Results of  $\alpha$  in  $ea_0^3$ ,  $\overline{\eta} = 10^{20} \times \eta$ , and  $\overline{\zeta} = 10^{17} \times \zeta$  for the ground state of Xe using different many-body methods. The estimated uncertainties to the CCSD<sub>p</sub>T calculations are given as  $\Delta$ .

Method of Evaluation	This work			Others			Ref.
	$\alpha$	$\overline{\eta}$	$\overline{\zeta}$	$\alpha$	$\overline{\eta}$	$\overline{\zeta}$	
DF	26.918	0.447	0.288	0.45	0.29		[25]
MBPT(2)	23.388	0.405	0.266				
MBPT(3)	18.693	0.515	0.339	0.52			[28]
CPHF	26.987	0.562	0.375	0.57	0.38		[25]
				27.7	0.564		[29]
LCCSD	27.484	0.608	0.417				
CCSD	27.744	0.501	0.336				
CCSD <sub>p</sub> T	27.782	0.501	0.337				
$\Delta$	0.050	0.002	0.004				
Experiment	27.815(27)						[27]

TABLE II. Explicit contributions to the  $\alpha$  in  $ea_0^3$ ,  $\overline{\eta} = 10^{20} \times \eta$ , and  $\overline{\zeta} = 10^{17} \times \zeta$  values from various CCSD<sub>p</sub>T terms.

Term	$\alpha$	$\overline{\eta}$	$\overline{\zeta}$
$\overline{D}T_1^{(1)} + \text{c.c.}$	26.246	0.506	0.338
$T_1^{(0)\dagger}\overline{D}T_2^{(1)} + \text{c.c.}$	0.008	$\sim 0$	$\sim 0$
$T_2^{(0)\dagger}\overline{D}T_2^{(1)} + \text{c.c.}$	1.395	-0.005	-0.001
Extra	0.095	$\sim 0$	-0.001

the basis functions which are given as  $\Delta$  in Table I. We estimate the contributions from the negative energy states using the Uehling potential [30], which is the lowest-order modified nuclear potential due to a virtual electron-positron pair. These contributions change  $\overline{\eta}$  from 0.501 to 0.503 and  $\overline{\zeta}$  from 0.337 to 0.338 at the CCSD<sub>p</sub>T level.

The results of calculations by others for  $\alpha$ ,  $\eta$ , and  $\zeta$  [25,28,29] as well as the methods used to calculate them are also given in Table I. As can be seen in that table, we have successfully reproduced the results of the previous calculations at the same level of approximation and we have gone beyond these approximations for obtaining accurate results. We present our results by performing the calculations using the MBPT(3), LCCSD, CCSD, and CCSD<sub>p</sub>T methods in Table I. These results provide useful insights into the role of different types of correlation effects. From the MBPT(3) calculations, we find that certain non-CPHF-type diagrams, for example, the diagrams shown in Fig. 1, contribute substantially with opposite signs to those of the DF values in all the above quantities, leading to large cancellations in the final results. Indeed, this is the main reason why the CPHF method overestimates the EDM enhancement factors compared to the CCSD<sub>p</sub>T method. In fact, many of these MBPT(3) diagrams correspond to the nonlinear terms of the CCSD<sub>p</sub>T method, hence their contributions are absent in the LCCSD method. Therefore, the LCCSD method also overestimates these results even though they account for some of the lower-order non-CPHF contributions.

We present the contributions from the individual CCSD<sub>p</sub>T terms in Table II to highlight the importance of various correlation effects. It can be seen in this table that by far

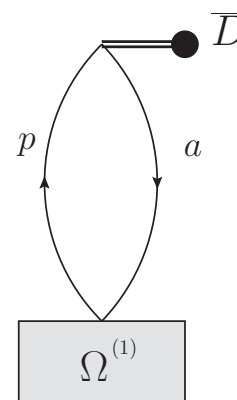


FIG. 2. Diagram involving effective one-body dipole operator  $\overline{D}$  and the perturbed wave operator  $\Omega^{(1)}$  that accounts for the contributions from the singly excited configurations.

TABLE III. Contributions from various matrix elements and from various angular momentum symmetry groups at the DF, lowest-order CPHF [denoted by MBPT( $l$ -CPHF)], CPHF, and CCSD $_p$ T methods to the  $\alpha$  in  $ea_0^3$ ,  $\bar{\eta} = 10^{20} \times \eta$ , and  $\bar{\zeta} = 10^{17} \times \zeta$  values. Here the summation indices  $n$  and  $m$  represent for the occupied and unoccupied orbitals, respectively.

Excitation(s) ( $a \rightarrow p$ )	DF			MBPT( $l$ -CPHF)			CPHF			CCSD $_p$ T		
	$\alpha$	$\bar{\eta}$	$\bar{\zeta}$	$\alpha$	$\bar{\eta}$	$\bar{\zeta}$	$\alpha$	$\bar{\eta}$	$\bar{\zeta}$	$\alpha$	$\bar{\eta}$	$\bar{\zeta}$
$5p_{1/2} - 7s$	0.248	0.030	0.007	0.336	0.056	0.016	0.380	0.062	0.016	0.352	0.050	0.014
$5p_{1/2} - 8s$	0.517	0.090	0.022	0.690	0.159	0.045	0.769	0.172	0.045	0.733	0.145	0.039
$5p_{1/2} - 9s$	0.237	0.106	0.025	0.284	0.166	0.044	0.301	0.174	0.044	0.309	0.157	0.041
$5p_{3/2} - 7s$	0.844	$\sim 0$	0.015	1.136	0.005	0.036	1.314	0.007	0.036	1.202	0.001	0.031
$5p_{3/2} - 8s$	1.558	$\sim 0$	0.043	2.056	0.014	0.093	2.351	0.018	0.093	2.261	0.024	0.082
$5p_{3/2} - 9s$	0.583	$\sim 0$	0.044	0.678	0.012	0.081	0.745	0.015	0.081	0.809	0.017	0.076
$5p_{1/2} - 7d_{3/2}$	2.267	$\sim 0$	$\sim 0$	2.200	-0.003	-0.008	2.407	-0.006	-0.008	2.259	-0.011	-0.008
$5p_{1/2} - 8d_{3/2}$	3.454	$\sim 0$	$\sim 0$	2.595	-0.013	-0.020	2.882	-0.022	-0.020	2.925	-0.028	-0.018
$5p_{3/2} - 7d_{5/2}$	5.667	$\sim 0$	$\sim 0$	5.747	-0.027	-0.018	6.365	-0.039	-0.018	5.827	-0.031	-0.018
$5p_{3/2} - 8d_{5/2}$	7.054	$\sim 0$	$\sim 0$	5.749	-0.048	-0.037	6.267	-0.071	-0.037	6.207	-0.057	-0.035
$\sum_{n,m}(ns - mp_{1/2})$	0.013	0.121	0.029	0.049	0.142	0.036	0.046	0.144	0.036	0.046	0.152	0.038
$\sum_{n,m}(ns - mp_{3/2})$	0.010	$\sim 0$	0.036	0.025	0.003	0.042	0.018	0.003	0.042	0.037	0.004	0.048
$\sum_{n,m}(np_{1/2} - ms)$	1.064	0.326	0.078	1.382	0.500	0.136	1.532	0.529	0.136	1.474	0.466	0.122
$\sum_{n,m}(np_{3/2} - ms)$	3.183	$\sim 0$	0.144	4.111	0.036	0.265	4.696	0.046	0.265	4.536	0.057	0.241
$\sum_{n,m}(np_{1/2} - md_{3/2})$	6.293	$\sim 0$	-0.001	4.993	-0.022	-0.033	5.582	-0.038	-0.033	5.539	-0.047	-0.031
$\sum_{n,m}(np_{3/2} - md_{3/2})$	1.545	$\sim 0$	$\sim 0$	1.326	-0.003	-0.006	1.501	0.003	-0.006	1.375	-0.006	-0.007
$\sum_{n,m}(np_{3/2} - md_{5/2})$	13.860	$\sim 0$	$\sim 0$	11.887	-0.082	-0.064	13.428	-0.125	-0.064	12.871	-0.099	-0.060

the most important contributions come from the  $\bar{D}T_1^{(1)}$  term followed by  $T_2^{(0)\dagger}\bar{D}T_2^{(1)}$ , where  $\bar{D}$  is the effective one-body term of  $\widehat{D}$  and the contributions from the other terms are almost negligible. To carry out an analysis similar to the one given in Ref. [29], we find the contributions from various orbitals that correspond to various singly excited intermediate configurations for different properties, which are given in Table III. These results are evaluated using the diagram shown in Fig. 2 with the corresponding  $\Omega^{(1)}$  operator from the DF, MBPT(2) containing diagrams that correspond only to the lowest-order CPHF [denoted by MBPT( $l$ -CPHF)], CPHF, and CCSD $_p$ T methods. We also present the sum of contributions from the orbitals belonging to a particular category of angular momentum excitations to demonstrate their importance in obtaining the properties that have been calculated. The information provided in all the three tables together clearly expounds the reasons for the different trends in the correlation effects in the calculations of  $\alpha$ ,  $\eta$  and  $\zeta$ .

By combining our CCSD $_p$ T results for  $\eta$  and  $\zeta$  with the available experimental limit for  $^{129}\text{Xe}$  EDM,  $d_a(^{129}\text{Xe}) <$

$4.1 \times 10^{-27} e \text{ cm}$ , we get the limits  $C_T < 1.6 \times 10^{-6}$  and  $S < 1.2 \times 10^{-9} e \text{ fm}^3$ . These are not superior to the limits extracted from  $^{199}\text{Hg}$  [25,31], which are about three orders of magnitude lower. However, the experiments on  $^{129}\text{Xe}$  [13,21,22] that are underway have the potential to improve the current sensitivity by about three to four orders of magnitude. It therefore seems very likely that the best limits for both  $C_T$  and  $S$  could be obtained by combining our calculated values presented in this work and the results of the new generation of experiments for  $^{129}\text{Xe}$  when they come to fruition. This limit for  $S$ , in conjunction with the recent nuclear structure calculations [32] and quantum chromodynamics (QCD), would yield new limits for  $\theta_{\text{QCD}}$  and  $CP$ -violating coupling constants involving chromo EDMs of quarks.

We acknowledge useful discussions with Professor K. Asahi. This work was supported in part by INSA-JSPS under Project no. IA/INSA-JSPS Project/2013-2016/February 28,2013/4098. The computations were carried out using the 3TFLOP HPC cluster at Physical Research Laboratory, Ahmedabad.

- [1] I. B. Khriplovich and S. K. Lamoreaux, *CP Violation Without Strangeness* (Springer, Berlin, 1997).
- [2] B. L. Roberts and W. J. Marciano, *Lepton Dipole Moments*, Advanced Series on Directions in High Energy Physics Vol. 20 (World Scientific, Singapore, 2010).
- [3] G. Liders, *Ann. Phys. (NY)* **281**, 1004 (2000).
- [4] J. H. Christenson, J. W. Cronin, V. L. Fitch, and R. Turley, *Phys. Rev. Lett.* **13**, 138 (1964).
- [5] K. Abe *et al.*, *Phys. Rev. Lett.* **87**, 091802 (2001).

- [6] B. Aubert *et al.*, *Phys. Rev. Lett.* **87**, 091801 (2001).
- [7] R. Aaij *et al.*, *Phys. Rev. Lett.* **110**, 221601 (2013).
- [8] M. Dine and A. Kusenko, *Rev. Mod. Phys.* **76**, 1 (2003).
- [9] M. Pospelov and A. Ritz, *Ann. Phys. (NY)* **318**, 119 (2005).
- [10] S. M. Barr, *Int. J. Mod. Phys. A* **8**, 209 (1993).
- [11] M. J. Ramsey-Musolf and S. Su, *Phys. Rep.* **456**, 1 (2008).
- [12] T. Furukawa *et al.*, *J. Phys.: Conf. Ser.* **312**, 102005 (2011).
- [13] T. Inoue *et al.*, *Hyperfine Interact.* **220**, 59 (2013).
- [14] E. T. Rand *et al.*, *J. Phys.: Conf. Ser.* **312**, 102013 (2011).

- [15] D. S. Weiss (private communication).
- [16] D. Heinzen (private communication).
- [17] S. M. Barr, *Phys. Rev. D* **45**, 4148 (1992).
- [18] W. C. Griffith *et al.*, *Phys. Rev. Lett.* **102**, 101601 (2009).
- [19] M. A. Rosenberry and T. E. Chupp, *Phys. Rev. Lett.* **86**, 22 (2001).
- [20] V. V. Flambaum, I. B. Khriplovich, and O. P. Sushkov, *Nucl. Phys. A* **449**, 750 (1986).
- [21] P. Fierlinger *et al.*, Cluster of Excellence for Fundamental Physics, Technische Universität München, <http://www.universe-cluster.de/fierlinger/xedm.html>
- [22] U. Schmidt *et al.*, Collaboration of the Helium Xenon EDM Experiment, Physikalisches Institut, University of Heidelberg, <http://www.physi.uni-heidelberg.de/Forschung/ANP/XenonEDM/Team>.
- [23] A. Yoshimi *et al.*, *Phys. Lett. A* **304**, 13 (2002).
- [24] V. V. Flambaum and J. S. M. Ginges, *Phys. Rev. A* **65**, 032113 (2002).
- [25] V. A. Dzuba, V. V. Flambaum, and S. G. Porsev, *Phys. Rev. A* **80**, 032120 (2009).
- [26] Y. Singh, B. K. Sahoo, and B. P. Das, *Phys. Rev. A* **88**, 062504 (2013).
- [27] U. Hohm and K. Kerl, *Mol. Phys.* **69**, 819 (1990).
- [28] A. M. Maartensson-Pendrill, *Phys. Rev. Lett.* **54**, 1153 (1985).
- [29] K. V. P. Latha and P. R. Amjith, *Phys. Rev. A* **87**, 022509 (2013).
- [30] E. A. Uehling, *Phys. Rev.* **48**, 55 (1935).
- [31] K. V. P. Latha, D. Angom, B. P. Das, and D. Mukherjee, *Phys. Rev. Lett.* **103**, 083001 (2009).
- [32] N. Yoshinaga, K. Higashiyama, R. Arai, and E. Teruya, *Phys. Rev. C* **87**, 044332 (2013).